Supplementary information for

Engineered extracellular matrices facilitate brain organoids from human pluripotent stem cells

Ayşe J. Muñiz, PhD,[1,2] Tuğba Topal, PhD,[1] Michael D. Brooks, PhD,[3] Angela Sze,[1] Do Hoon Kim, PhD,[1,4] Jacob Jordahl, PhD,[1,4] Joe Nguyen, PhD,[1] Paul H. Krebsbach, DDS, PhD,[1] Masha G. Savelieff,[5,6] Eva L. Feldman, MD, PhD,[5,6,*] Joerg Lahann, PhD[1,2,4,*]

[1]Biointerfaces Institute, University of Michigan, Ann Arbor, MI, USA

[2]Macromolecular Science and Engineering Program, University of Michigan, Ann Arbor, MI, USA

[3]Department of Internal Medicine, University of Michigan, Ann Arbor, MI, USA

[4]Department of Chemical Engineering, University of Michigan, Ann Arbor, MI, USA

[5]NeuroNetwork for Emerging Therapies, University of Michigan, Ann Arbor, MI, USA

[6]Department of Neurology, University of Michigan, Ann Arbor, MI, USA

*Correspondence to:

Joerg Lahann, PhD; ORCID 0000-0002-3334-2053; NCRC Building 10, Room A175, 2800 Plymouth Rd, Ann Arbor, MI 48109; Phone: (734) 763-7924; Email: lahann@umich.edu.

Eva L. Feldman, MD, PhD; ORCID 0000-0002-9162-2694; 5017 AAT-BSRB, 109 Zina Pitcher Place, Ann Arbor, MI 48109; Phone: (734) 763-7274; Email: efeldman@umich.edu.

Contents

Materials and Methods

Fabrication of engineered extracellular matrices

EECMs are a composite material of synthetic polymer and human-derived protein. EECMs were fabricated as previously described.[1,2] A highly porous polymer structure was generated by 3D jet writing and then placed between two medical-grade stainless steel frames with window cut-outs and secured with 1 µL of acrylate adhesive (Loctite, Rocky Hill, CT). 3D jet writing is a modified electrospinning process, which we performed using a custom apparatus. The apparatus was comprised of equipment used to deposit the polymer fibers, and equipment used to control the fiber deposition process. The fiber deposition equipment included: a mechanical pump and a polymer-containing syringe and needle coupled to an electrode. The syringe contains 500 µL of a polymer solution of poly(D,L-lactide-co-glycolide) (PLGA) 85:15 (Millipore Sigma, St. Louis, MO) in 0.93:0.07 volume fraction chloroform:N,N-dimethylformamide at a 0.3 w/v fraction of polymer to solvent. The equipment used to control the fiber deposition includes: an electrically grounded collecting plate located on two motion stages which are controlled by a 4-axis controller linked to LabView software, and a copper ring secondary electrode which acts as an electrical lens to focus a single microfiber toward the collection plate. Using a DC power supply (Gamma High-Voltage Research ES30P-20W), we applied a positive potential to induce electrospinning of the microfiber. The range of the potential of the needle capillary was approximately 11-14 kV while the ring electrode was approximately 7-9 kV. The LabView software was programmed to generate woven fiber stacks that produce 500 µm pores of 10 polymer fiber layers over a 14 x 14 mm area. Once the polymer fibers were done depositing, we removed them from the collection plates and placed them under vacuum for 2 weeks to remove residual solvent. Sterilization was achieved through UV exposure and brief 70% EtOH treatment. To create EECMs of fibrillar FN, this scaffolding is placed in a plasma fibronectin solution (Corning, Glendale, AZ) diluted in DPBS with no magnesium or calcium (Gibco, Grand Island, NY) to a concentration of 0.111 mg/mL and then tumbled in a microcentrifuge tube at 8 RPM in a 30 ºC chamber for at least two hours. The air-polymer-protein interface induces fibrillogenesis of the fibronectin to convert the soluble protein to insoluble protein fibrils.[2,3] The resulting structure is an ultra porous polymer scaffold laden with a fibrillar fibronectin protein matrix, referred to collectively as EECM.

Stem cell culture

Two hPSC sources were used in this study. H9 (WA09) embryonic stem cells were originally from WiCell (Madison, Wisconsin) and were a gift from the lab of Paul Krebsbach (The University of Michigan, Ann Arbor, MI). iPSC 19-9-11 cells were provided from the University of Michigan Cardiovascular and Regeneration Core (Ann Arbor, MI). Both cells were maintained and passaged on Matrigel-coated plates and were below passage 40. H9 cells were cultured in StemFlex media (Thermo Fisher), and iPSC were maintained in StemMACS iPS-Brew XF, human (Miltenyi Biotec). These cells were maintained at 37 ºC in a humidified incubator with 5% CO_2. The cells were passaged weekly with picking to remove or keep unwanted cells to maintain highly pure populations of pluripotent stem cells. Desirable properties include cells that were polygonal in shape, homogenous with sharp borders, and a high nucleus to cytoplasm ratio. Differentiated cells were mechanically removed using a sterile pulled-glass pipet under a stereomicroscope (LeicaMZ9.5, Leica Microsystems Inc., Buffalo Grove, IL).

Generation of Matrigel and EECM-based neural cultures

Stem cells were seeded and expanded using two methods, either Matrigel or EECM expansion. hPSCs were dissociated from Matrigel to single cells using Accutase and cell-scraping with 10 μM ROCK inhibitor Y27632 (Calbiochem). Cells were then seeded either back to Matrigel or on EECMs to carry out differentiation. To compare Matrigel and EECM protocols as consistently as possible, Matrigel neural progenitor cells were cultured in the absence of embryoid body formation as we did not generate embryoid bodies prior to EECM seeding. We followed the monolayer protocol provided by StemCell Technologies in products cat# 05839 and cat# 08522. The manufacturer media changing instructions were adhered to for both Matrigel and EECMs, with noted exceptions. For EECM-supported organoids only, hPSC single cells were seeded onto EECMs that were placed in an ultra-low attachment 24-well plate (Corning product cat# CLS3473). The cells were allowed to attach overnight and then rinsed to remove unattached cells using feeder-free medium. The cells were allowed to expand until they reached confluency (about five days on average). Once a confluent monolayer of cells was achieved, the transition to differentiation media was performed. Cells were exposed to Neural Induction Medium for 7 days, Midbrain Neuron Differentiation media medium for 14 days (we note the lack of disassociating cells from their niches, per suggested in the manufacturer protocol), Midbrain Neuron Maturation medium (MNM-1) for 6 days, and Midbrain Neuron Maturation medium (MNM-2) until collection (minimum of 14 days, up to 154 days).

Immunofluorescence staining and microscopy

Early time point EECM-supported organoid samples were fixed using Z-fix (10% aqueous buffered zinc formalin) (Anatech, LTD) overnight and rinsed 3X in DPBS. The samples were blocked with 1% BSA and 0.5% Triton-X-100 in PBS for 1 hour at room temperature. The samples were incubated with primary antibodies overnight and secondary antibodies for 1 hour, with 3X DPBS wash steps between staining stages. The samples were imaged on a Nikon Instruments A1 Confocal Laser microscope with NIS-Elements C Software. Images were processed using Imaris image analysis software. Brightfield images were taken using an Olympus IX83 microscope (Biointerfaces Institute, University of Michigan, Ann Arbor, MI). All primary antibodies were used as outlined in **Table 1** with a working volume of 1 mL in 5% BSA in PBS, unless noted otherwise.

Table 1. Primary antibody list for immunofluorescence staining

Target	Company cat#	Dilutions/ Concentration	Species
Oct 3/4	SCBT cat# sc8629	1:500	Goat
Nanog	Abcam cat# ab62734	1:100	Mouse
Sox2	Millipore cat# ab5603	1:500	Rabbit
ZO-1 (D6L1E)	CST cat# 13663	1:500	Rabbit
Pax6	SCBT cat# sc81649	1:500	Mouse

Sox1	RnD cat# AF3369	10 µg/mL	Goat
Beta-catenin	CST cat# 8480	1:100	Rabbit
TUJ1 (TUBB3)	CST cat# 5568S	1:200	Rabbit
OTX2	RnD cat# AF1979	5 µg/mL	Goat
Synaptophysin (7H12)	CST cat# 9020	1:200	Mouse
Map2	CST cat# 4542	1:50	Rabbit

Secondary antibodies for immunofluorescence: All antibodies were used at a concentration of 1:1,500 with a working volume of 1.5 mL in 5% BSA in PBS. DAPI stain was used for DNA. Donkey anti-Mouse IgG Secondary Antibody, Alexa Fluor® 488 (TFS: cat# R37114). Donkey anti-Rabbit IgG Secondary Antibody, Alexa Fluor® 594 (TFS: cat# A-21207).

Western blot analysis

Cells were collected and lysed in NP40 lysis buffer (NaCl at 150 mM, NP-40 at 1.0%, and TrisCl at 50 mM, pH 8.0). Supernatant was quantified using Bio-Rad Protein Assay (Bio-Rad; cat# 5000006) with the Biotek Nova Spectrophotometer at 595 nm wavelength. 10 µg of protein lysate was mixed with 3x Laemmli loading buffer (4% SDS, 10% 2-mercaptoethanol, 20% glycerol, 0.004% bromophenol blue, 0.125 M Tris-HCl, brought to pH 6.8). Novex® Tris-Glycine SDS Running Buffer 10X (TFS: cat# LC2675-4) was diluted to 1X with milliQ filtered deionized water. We used Novex™ WedgeWell™ 4–20% Tris-Glycine Gels (TFS; cat# XP04205BOX) and XCell SureLock® Mini-Cell (TFS; cat# EI0001). Precision Plus Protein™ Dual Color Standards (Bio-Rad; cat# 1610374) to approximate molecular weights from 10 kDa to 250 kDa. Gels are run at 150 V for 85 min. For transfer of proteins, Trans-Blot® SD Semi-Dry Transfer Cell (Bio-Rad; cat# 170-3940) was used and PVDF membranes dipped in methanol briefly and rinsed in 1X Transfer Buffer (25 mM Tris, 192 mM glycine, 20% methanol (v/v), 0.5% SDS at pH 8.3) (Bio-Rad; cat# 162-0177 R) to transfer 24 V for 60 min. After the transfer, membranes were blocked for 30 min in a 2.5% blocking solution (Bio-Rad; cat# 1706404) in 50 mL 1X TBST (50 mM Tris-Cl, pH 7.5, 150 mM NaCl, Tween-20 (FS; cat# BP337-100) for 30 min, followed by 1x wash for 30 min in 1X TBST. Prior to antibody incubation, membranes were cut between the 75 kDa and 100 kDa bands to optimize for proteins above 100 kDa in size, above 75 kDa and above the 37 kDa membrane for proteins within those ranges, and between 20–25 kDa for proteins above and below those ranges. This allows for optimal antibody incubation with the proper membranes. After incubating membranes in primary antibodies overnight at 4 °C, they were washed for 30 min in 1X TBST at room temperature (RT), shaking. Next, membranes were incubated in the appropriate secondary antibody for one hour and washed for 30 min in 1X TBST at RT. For film capture, membranes were incubated with SuperSignal™ West Pico Chemiluminescent Substrate (TFS; cat# 34078) for 3 min at RT. We used HyBlot CL autoradiography film (Denville Scientific: cat# e3018).

Almost all antibodies were purchased from Cell Signaling Technologies (CST) (**Table 2**). Primary antibodies were used at 1:1,000 dilution in 5% BSA in 1X TBST buffer with 0.04% sodium azide. GAPDH was used for loading controls.

Table 2. Primary antibody list for Western blot

Target	Company cat#	MW	Species
Oct 3/4	CST cat# 2750S	45	Rabbit
Nanog (D73G4)	CST cat# 4903	42	Rabbit
E-cadherin (4A2)	CST cat# 14472	135	Mouse
N-cadherin (D4R1H)	CST cat# 13116	140	Rabbit
Nestin	CST cat# 33475	207	Mouse
Sox1	CST cat# 4194S	40	Rabbit
BRN2	CST cat# 12137	55	Rabbit
TUJ1	CST cat# 5568S	55	Rabbit
p-YAP (S127)	CST cat# 13008S	65-78	Rabbit

***Secondary antibodies for immunoblot analysis*:** 1:4,000 dilution for α-mouse IgG (H + L) HRP conjugate (Promega; cat# W4021). 1:7,500 dilution for α-rabbit IgG (H + L) HRP conjugate (Promega; cat# W4011).

Single-cell sequencing library generation

Drop-Seq was performed as described in Macosko, *et al*.[4] Briefly, cells were resuspended in BSA at 100 cells/μL in 0.01% BSA in PBS. Oligo labeled beads from Chemgenes were resuspended in lysis buffer at 120 beads/μL. Labeled beads and cells were processed through the standard Drop-Seq device (FlowJEM) for 10 minutes per sample. Beads were collected and approximately 1000 cell-bead pairs (STAMPs) per sample were put into a reverse transcription reaction, followed by an Exonuclease I step, and then universal PCR. Results from the PCR were quantified on a Bioanalyzer DNA high sensitivity chip. 1.5 ng of amplified cDNA from each sample was used in a tagmentation step using generated Tn5 transposase as described by Picelli *et al.*[5] After tagmentation, samples were loaded onto Illumina HiSeq sequencers.

Single-cell sequencing data analysis

The computational processing pipeline from Macosko *et al.*[4] (version 1.2) was followed to map raw Illumina reads to the human genome (hg19) using STAR as the aligner to generate digital gene expression matrices. Digital gene expression files were then subsequently processed with the package Scanpy (version 1.4.2)[6] using Python (version 3.6.8). These data underwent processing based on current standards in the field, described in further detail here referencing the specific software functions used.[7,8] Samples underwent quality control steps and were filtered based on having min_genes = 500 and min_cells = 5. The normalization and filtering steps then followed the recipe of Zheng, *et al.*[9] keeping all top genes expressed to minimize bias between samples. The samples were further filtered to have n_genes_by_counts < 4500. Cells were filtered based on cells having below 30% mitochondrial gene expression and > 5%

ribosomal gene expression. Normalization per cell occurred at a depth of 10,000 counts and then were log transformed. The cell cycle phase for each cell was identified based on scoring gene expression of genes related to the cell cycle identified by Tirosh*, et al.*[10] The data were linearly regressed on the basis of the total_counts as identified by the calculate_qc_metrics function. Principal component analysis was ran and the variance ratio was used to identify the number of principal components to use in calculating the neighborhood graph using the Scanpy neighbors function (20 principal components, 10 neighbors). UMAP[11] was used to visualize the Leiden[12] clusters in two-dimensional graphs. Pathway scoring was achieved using the score_genes function, which is the average expression of a set of provided genes subtracted with the average expression of a randomly sampled set of reference genes of the same size for lists ≥ 50. The reference list was set to 50 if the provided gene set was less than 50 genes long. Pathways genes were identified using the GO database (Supplementary Table S4).[13,14] Cell identities for each Leiden cluster were made on the basis of the differential gene expression for each cluster using the rank_genes_groups function in Scanpy. Canonical marker genes used to identify clusters were assembled from recent work by Tanaka, *et al*.[15] and Pollen, *et al.*[16] (Supplementary Table S5). Comparison of expression counts between groups was performed on processing pipeline-matched samples. The entropy index was calculated on filtered and non-log transformed, unregressed data following the recipe of Chen, *et al.* using the SCENT package in R Studio.[17,18]

Mass spectrometry

Samples were buffer exchanged and concentrated to ~60 µL on a Corning SpinX 5Kd MWCO filter. The protein concentration of the concentrated material was determined by Qubit fluorometry. 20 µg of each sample was processed by SDS-PAGE using a 10% Bis-Tris NuPage Mini-gel with the MES buffer system (Invitrogen). The gel was run 5 cm and each gel lane was excised into twenty equally sized bands. Gel bands were processed by in-gel digestion with trypsin using a ProGest robot (DigiLab). The samples were washed with 25 mM ammonium bicarbonate followed by acetonitrile. They were educed with 10 mM dithiothreitol at 60°C followed by alkylation with 50 mM iodoacetamide at room temperature (RT). Samples were then digested with sequencing grade trypsin (Promega) at 37 °C for 4 h. Quenching was done with formic acid and analyzed without further processing.

Half of each digest was analyzed by nano LC-MS/MS with a Waters NanoAcquity HPLC system interfaced to a Thermo Fisher Fusion Lumos mass spectrometer. Peptides were loaded on a trapping column and eluted over a 75 µm analytical column at 350 nL/min using a 0.5 h reverse phase gradient; both columns were packed with Luna C18 resin (Phenomenex). The mass spectrometer was operated in data-dependent mode with the Orbitrap operating at 60,000 FWHM and 15,000 FWHM for MS and MS/MS respectively. The instrument was run with a 3 s cycle for MS and MS/MS with Advanced Peak Determination (APD) enabled. A total of 10 h of instrument time per sample was employed.

Proteomics analysis

Data were searched using a local copy of Mascot with the following parameters:

Enzyme: Trypsin/P

Database: SwissProt Human (concatenated forward and reverse plus common contaminants)

Fixed modifications: Carbamidomethyl (C),

Variable modifications: Oxidation (M), Acetyl (N-term), Pyro-Glu (N-term Q), Deamidation (N,Q)

Mass values: Monoisotopic

Peptide Mass Tolerance: 10 ppm

Fragment Mass Tolerance: 0.02 Da

Max Missed Cleavages: 2

Signatures were compared to previously published cerebrospinal fluid data acquired provided in Pellegrini, *et al.*[19] Filtering for proteins to include in the interaction analysis was based on at least two EECM-supported brain organoids having an emPAI ≥ 1. We use the interactiVenn tool[20] to survey the interaction of proteins. The protein lists were passed into PantherDB[21] and the Reactome database[22] for analysis.

Extraction and purification of total RNA

Scaffolds and Matrigel coated plates were washed with PBS, then 1000 µL of Trizol Reagent (Invitrogen, Carlsbad, CA) was added to both substrates. RNAs were collected after brisk pipetting and 200 µL Chloroform was added to this solution. Then, it was centrifuged for 13,000 g-15 min. Aqueous phase containing RNA was separated and collected from the solution. 500 µL isopropanol was added to this aqueous phase and stored at 20 °C. Then, the manufacturer's RNA Clean-up protocol, RNeasy Mini-Kit (Qiagen, Valencia, CA), with the optional On-column DNAse treatment was followed. RNA quality and concentration were checked using a Synergy NEO HTS Multi-Mode Microplate Reader (BioTek Instruments, Winooski, VT).

Quantitative qPCR analysis

Reverse transcription from 2.5 µg of total RNA in a 20 µL reaction into cDNA was performed using SuperScript™ VILO™ Master Mix (Thermo Fisher cat# 11755050). The synthesis of first-stranded cDNA was carried out in the PCR tube after combining SuperScript VILO, RNA, and DEPC-treated water, in the first cycle at 25 °C for 10 min, incubating at 42 °C for 60 min, and terminating the reaction at 85 °C for 5 min. Quantitative PCR was performed triplicate for each sample using TaqMan probes (Applied Biosystems) and TaqMan Universal PCR Master Mix (Applied Biosystems) on 7900 HT Fast Real Time PCR system (Applied Biosystems). Relative quantification of *LMX1A*, *FOXA2*, *FGF8*, *TUJ1*, *OTX2*, *SYP* (synaptophysin) gene expression data were normalized to the GAPDH expression and calculated using the $2^{-\Delta\Delta CT}$ method. The list of primers used in qPCR is in **Table 3**. All primers were purchased from Thermo Fisher Life Technologies.

Table 3. List of primers used in qPCR

Gene of Interest	Assay ID	Cat #	UniGene ID
FOXA2	Hs00232764_m1	4331182	Hs.155651
LMX1A	Hs00898455_m1	4331182	Hs.667312
OTX2	Hs00222238_m1	4331182	Hs.288655
TUJ1	Hs00801390_s1	4331182	Hs.511743
SYP	Hs00300531_m1	4331182	Hs.632804
GAPDH	Hs02786624_g1	4331182	Hs.544577

Statistical analysis

Statistics were performed in Python (version 3.6.8) using the SciPy package.[23] Pairwise comparison tests were chosen based on tests for normality (Shapiro-Wilk's test) and variance (Levene's test). On this basis, unless otherwise specified, we selected the nonparametric Mann Whitney U test ('wilcoxon' in Scanpy) to evaluate statistical significance between two groups. For pathways analysis, we used g:Profiler[24] to perform functional enrichment analysis on supplied gene lists which were selected on the basis of being upregulated relative to another group with an adjusted p-value < 0.05 as assessed by the rank_genes_group function in Scanpy,[6] with Benjamini-Hochberg correction unless noted otherwise. All statistics were run on data replicates derived from distinct samples.

SUPPLEMENTARY FIGURES

Supplementary Figure S1. Extended analysis of EECM and Matrigel (MG) supported organoids after Neural Induction Medium. a MG and EECM samples were clustered using the Leiden algorithm and plotted using UMAP to visualize cluster distribution, with the clusters quantified in the right panel. **b** Samples were categorized by their distribution in the cell cycle phase. **c, d** Pathways analysis was performed using g:Profiler[24] for the top 200 differentially expressed genes (p ≥ 0.01) upregulated in EECM-supported organoids (c) and MG-supported organoids (d). **e** Scores were computed for pathways. * denotes the higher mean group assessed by Mann Whitney U alternative (one-tailed) testing.

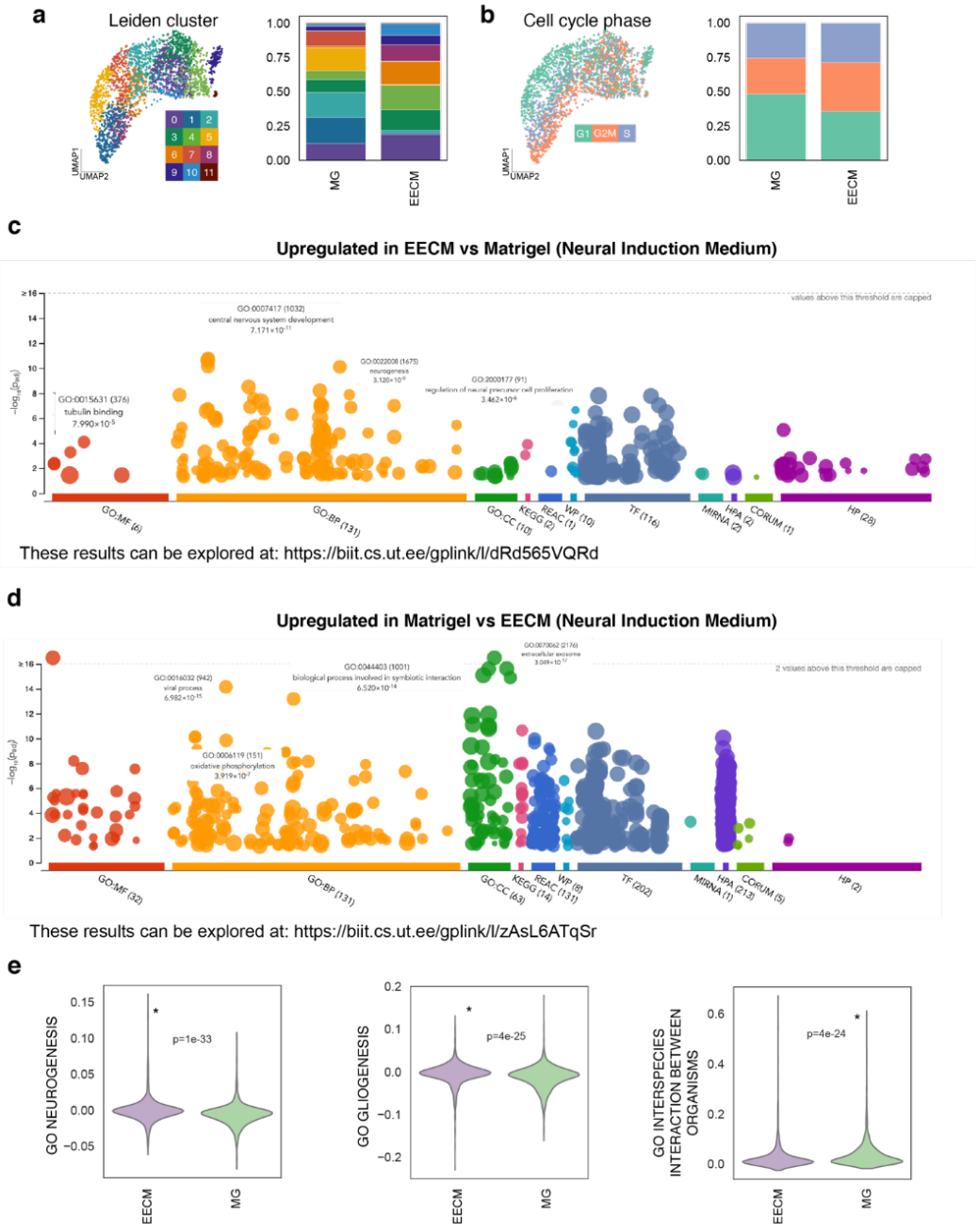

Supplementary Figure S2. Analysis of apoptosis in EECM-supported brain organoids. **a** Barplot representing a cumulative pathway score for the Hallmark Apoptosis gene set as described in the GO database,[13,14] calculated for the 47-day maturation of EECM and Matrigel ("MG") organoids. We benchmarked the score against previously published iPSC-derived Neurons that were either treated with rotenone, a toxic pesticide used to induce Parkinson's disease-like symptoms in neurons, or untreated.[25] **b** Reactome database[22] analysis of protein signatures from proteomics from late-stage EECM organoids. Visualization shows pathways nested under "Programmed Cellular Death," "Cellular Response to Stimuli," and "Extracellular Matrix Organization" for comparison. P-values represent significance of pathway overrepresentation (bright yellow = 0; dark yellow = 0.05; grey > 0.05).

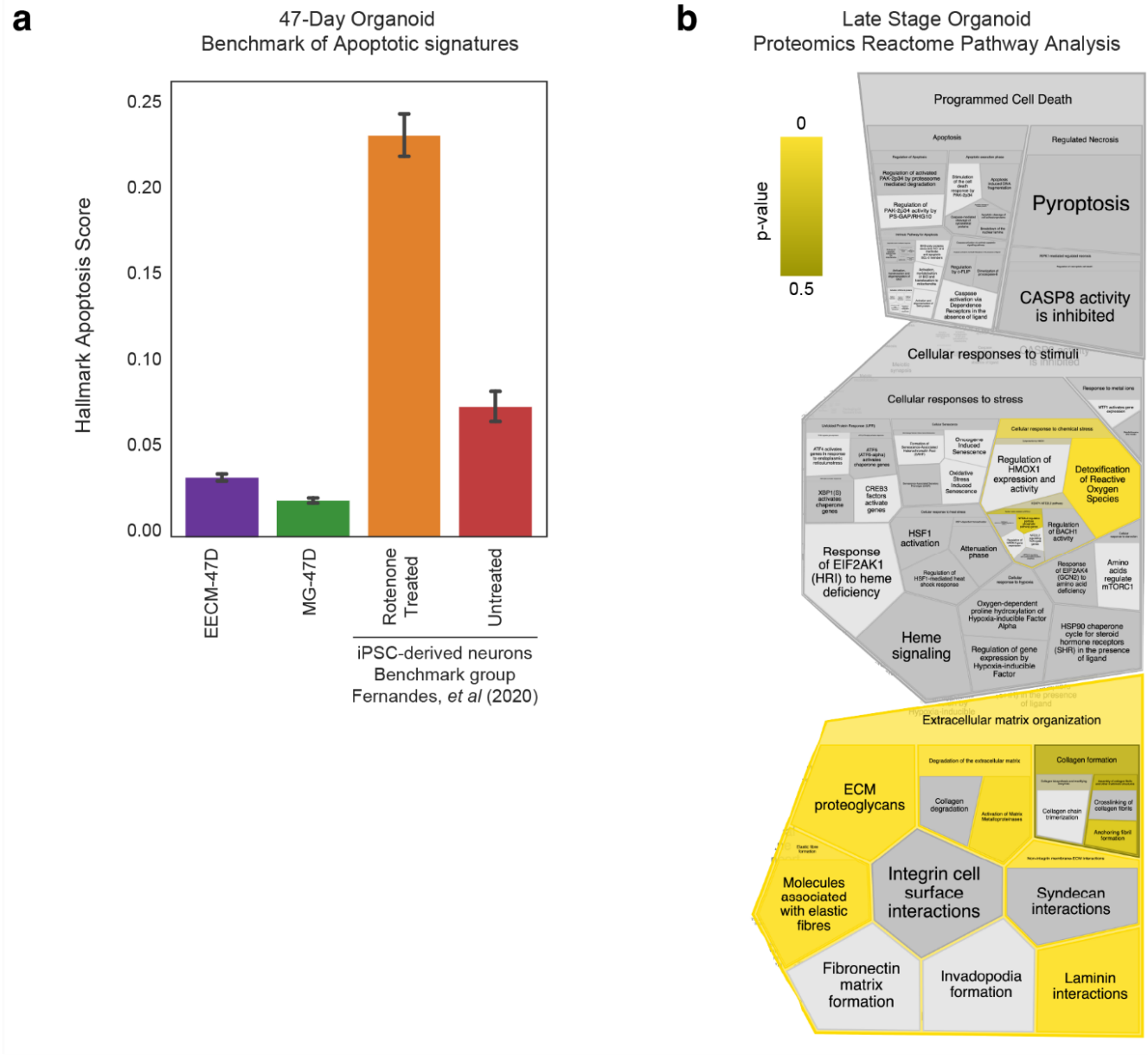

Supplementary Figure S3. a Pathways analysis using g:Profiler[24] for proteomics signatures observed in extended culture EECMs (emPAI ≥ 1 in at least 2 organoids). **b** Top Gene Ontology pathways are shown along with the calculated adjusted p-value. These results may be explored online at https://biit.cs.ut.ee/gplink/l/7s1qB0NeS7.

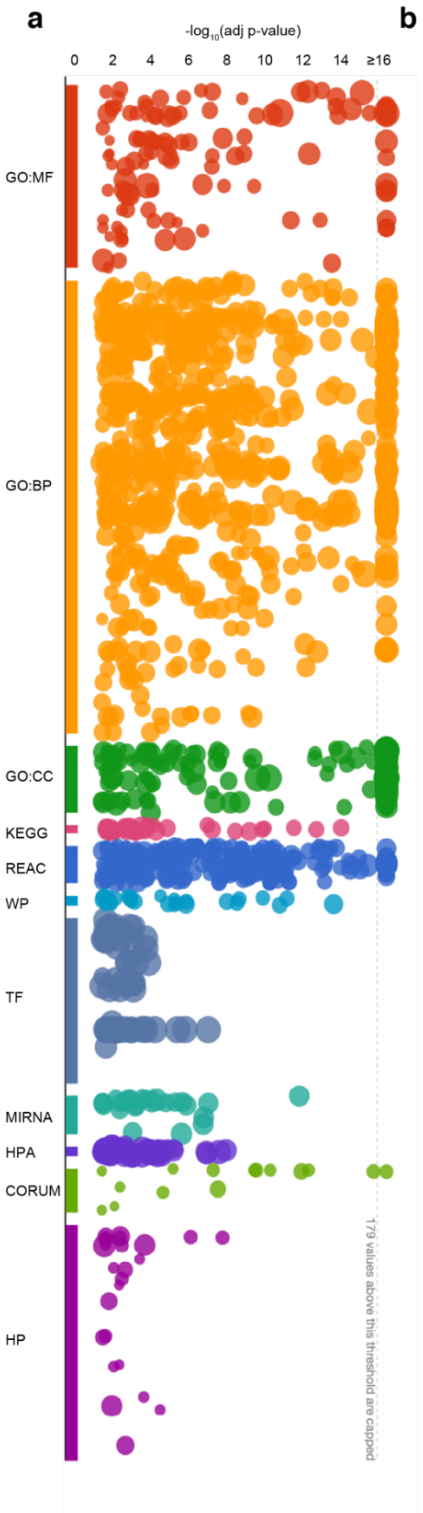

b

Gene Ontology term name	Term ID	p_{adj}	$-\log_{10}$(adj p-value)
structural molecule activity	GO:0005198	2.375×10^{-64}	
cell adhesion molecule binding	GO:0050839	6.007×10^{-55}	
extracellular matrix structural constituent	GO:0005201	7.461×10^{-50}	
protein-containing complex binding	GO:0044877	2.586×10^{-41}	
cadherin binding	GO:0045296	3.641×10^{-31}	
identical protein binding	GO:0042802	2.829×10^{-28}	
protein binding	GO:0005515	1.684×10^{-27}	
peptidase regulator activity	GO:0061134	4.770×10^{-26}	
endopeptidase regulator activity	GO:0061135	1.651×10^{-22}	
endopeptidase inhibitor activity	GO:0004866	2.881×10^{-22}	
enzyme inhibitor activity	GO:0004857	1.267×10^{-21}	
peptidase inhibitor activity	GO:0030414	1.667×10^{-21}	
peptidase activity	GO:0008233	2.083×10^{-20}	
calcium ion binding	GO:0005509	2.345×10^{-20}	
integrin binding	GO:0005178	8.424×10^{-20}	
hydrolase activity	GO:0016787	1.514×10^{-19}	
glycosaminoglycan binding	GO:0005539	7.046×10^{-18}	
collagen binding	GO:0005518	2.553×10^{-16}	
catalytic activity	GO:0003824	6.344×10^{-16}	
signaling receptor binding	GO:0005102	2.430×10^{-15}	
heparin binding	GO:0008201	1.204×10^{-14}	
endopeptidase activity	GO:0004175	1.497×10^{-14}	
serine-type endopeptidase inhibitor activity	GO:0004867	1.620×10^{-14}	
sulfur compound binding	GO:1901681	2.577×10^{-14}	
regulated exocytosis	GO:0045055	2.704×10^{-82}	
exocytosis	GO:0006887	8.117×10^{-78}	
neutrophil mediated immunity	GO:0002446	1.107×10^{-77}	
neutrophil activation involved in immune response	GO:0002283	1.620×10^{-76}	
neutrophil degranulation	GO:0043312	2.801×10^{-76}	
neutrophil activation	GO:0042119	1.777×10^{-74}	
granulocyte activation	GO:0036230	1.739×10^{-73}	
myeloid leukocyte mediated immunity	GO:0002444	1.661×10^{-72}	
leukocyte degranulation	GO:0043299	1.414×10^{-69}	
myeloid cell activation involved in immune response	GO:0002275	1.068×10^{-68}	
secretion by cell	GO:0032940	2.477×10^{-64}	
secretion	GO:0046903	8.079×10^{-64}	
myeloid leukocyte activation	GO:0002274	3.121×10^{-61}	
export from cell	GO:0140352	5.816×10^{-61}	
immune effector process	GO:0002252	8.324×10^{-59}	
cell activation involved in immune response	GO:0002263	2.267×10^{-57}	
establishment of localization in cell	GO:0051649	2.385×10^{-57}	
leukocyte activation involved in immune response	GO:0002366	3.465×10^{-56}	
leukocyte mediated immunity	GO:0002443	1.578×10^{-55}	
vesicle-mediated transport	GO:0016192	1.526×10^{-53}	
organonitrogen compound metabolic process	GO:1901564	5.491×10^{-48}	
cell activation	GO:0001775	5.965×10^{-47}	
external encapsulating structure organization	GO:0045229	8.606×10^{-45}	
catabolic process	GO:0009056	1.026×10^{-44}	
cellular localization	GO:0051641	3.254×10^{-44}	
extracellular matrix organization	GO:0030198	1.334×10^{-42}	
extracellular space	GO:0005615	4.941×10^{-324}	
extracellular organelle	GO:0043230	4.941×10^{-324}	
extracellular vesicle	GO:1903561	4.941×10^{-324}	
extracellular exosome	GO:0070062	4.941×10^{-324}	
extracellular membrane-bounded organelle	GO:0065010	4.941×10^{-324}	
extracellular region	GO:0005576	2.267×10^{-298}	
vesicle	GO:0031982	1.925×10^{-251}	
secretory granule lumen	GO:0034774	6.517×10^{-92}	
vesicle lumen	GO:0031983	9.653×10^{-92}	
cytoplasmic vesicle lumen	GO:0060205	5.380×10^{-91}	
collagen-containing extracellular matrix	GO:0062023	1.176×10^{-89}	
secretory granule	GO:0030141	2.408×10^{-88}	
extracellular matrix	GO:0031012	5.980×10^{-79}	
external encapsulating structure	GO:0030312	8.138×10^{-79}	
secretory vesicle	GO:0099503	1.803×10^{-78}	
cytoplasm	GO:0005737	1.630×10^{-62}	
cytoplasmic vesicle	GO:0031410	5.796×10^{-54}	
ficolin-1-rich granule lumen	GO:1904813	6.409×10^{-54}	
intracellular vesicle	GO:0097708	9.365×10^{-54}	
cytosol	GO:0005829	4.791×10^{-53}	
ficolin-1-rich granule	GO:0101002	1.108×10^{-52}	
membrane-bounded organelle	GO:0043227	1.967×10^{-50}	
cell-substrate junction	GO:0030055	2.843×10^{-49}	

Supplementary Figure S4. Comparison of EECM-organoids to CHIR/BMP4 patterned ChP organoids. a Interaction Venn diagram[20] generated to visualize overlapping terms for proteomics signatures found in CSF derived from adult, pediatric, embryonic, choroid plexus (ChP) organoids,[19] and EECM-supported organoids (this study). **b** PantherDB was used to identify pathways overlap between the CSF of adult, ChP, and EECM samples (Supplementary Table S10). **c** Reactome[22] was used to visualize the biological processes that overlap between the ChP (orange) and EECM (purple) supported organoids.

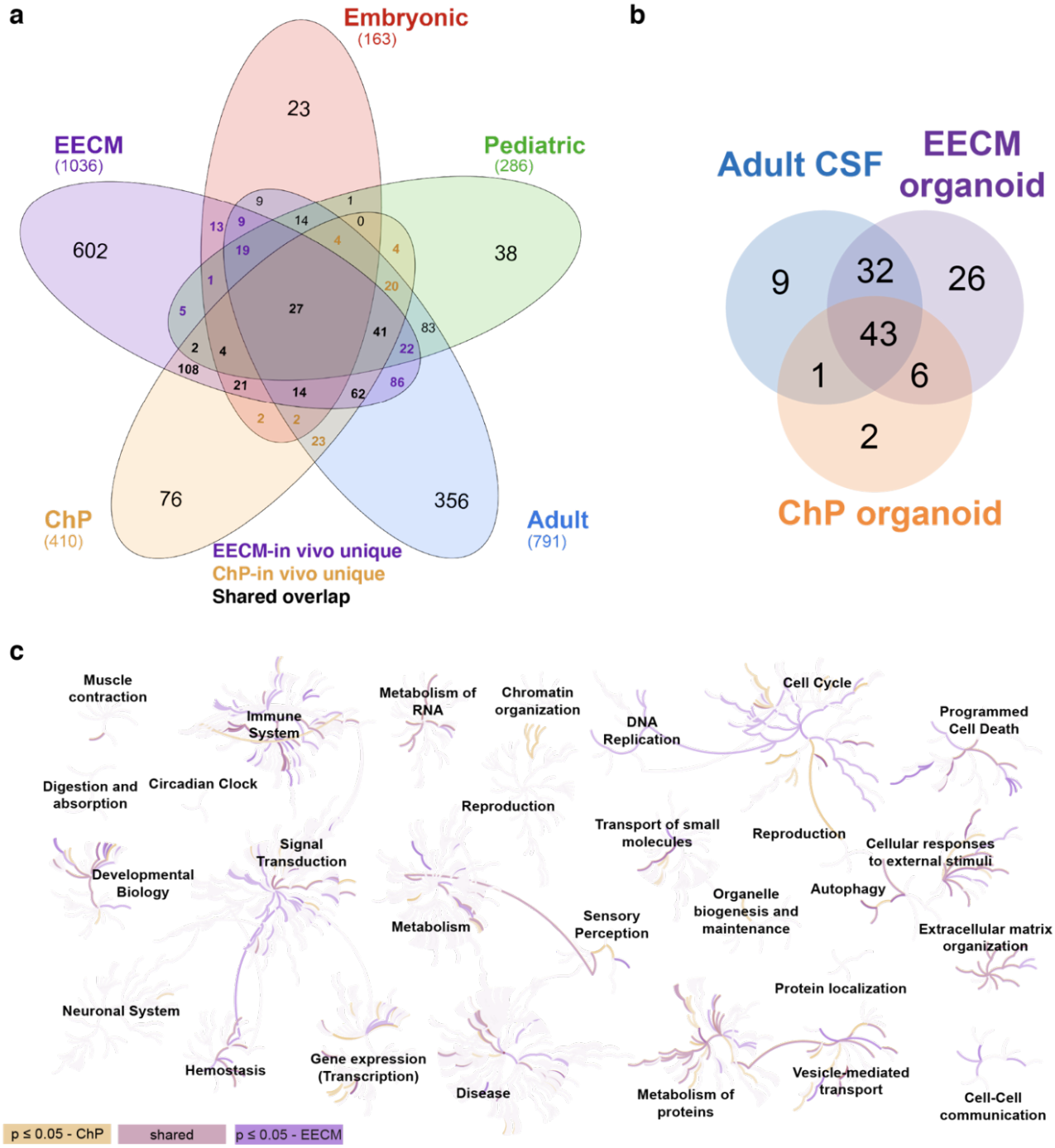

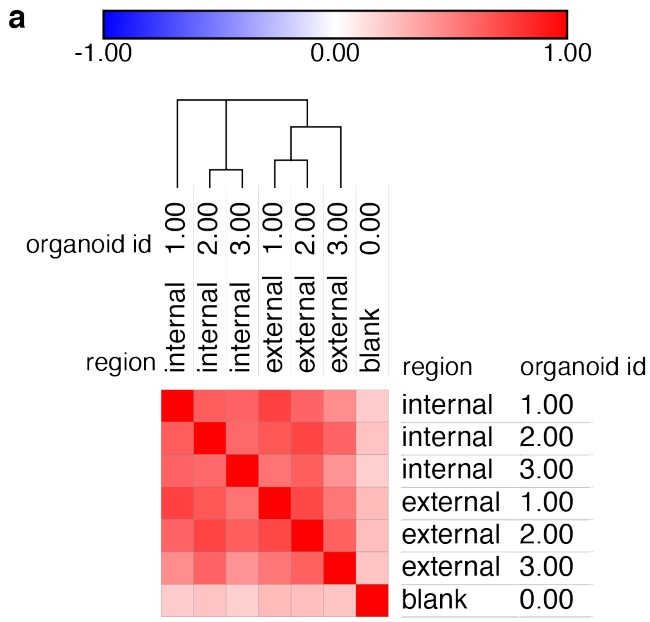

Supplementary Figure S5. Proteomic comparison of organoid batches shows high batch-to-batch consistency. a Spearman rank correlation calculation based on quantitative mass spectrometry data with hierarchical clustering based on region. Region identifies whether the mass spectrometry was performed on media from inside the organoid ("internal"), outside the organoid ("external"), or without organoids ("blank"). The identity of the organoid ("id") specifies from which organoid batch the sample was derived.

References

1. Jordahl JH, Solorio L, Sun H, et al. 3D Jet Writing: Functional Microtissues Based on Tessellated Scaffold Architectures. *Adv Mater*. Apr 2018;30(14):e1707196. doi:10.1002/adma.201707196
2. Jordahl S, Solorio L, Neale DB, et al. Engineered Fibrillar Fibronectin Networks as Three-Dimensional Tissue Scaffolds. *Adv Mater*. Nov 2019;31(46):e1904580. doi:10.1002/adma.201904580
3. Neale DB, Muñiz AJ, Jones MS, et al. Aligned Networks of Engineered Fibrillar Fibronectin Guide Cellular Orientation and Motility. *Small Structures*. 2021;2(6):2000137. doi:https://doi.org/10.1002/sstr.202000137
4. Macosko EZ, Basu A, Satija R, et al. Highly Parallel Genome-wide Expression Profiling of Individual Cells Using Nanoliter Droplets. *Cell*. May 21 2015;161(5):1202-1214. doi:10.1016/j.cell.2015.05.002
5. Picelli S, Faridani OR, Björklund AK, Winberg G, Sagasser S, Sandberg R. Full-length RNA-seq from single cells using Smart-seq2. *Nat Protoc*. Jan 2014;9(1):171-81. doi:10.1038/nprot.2014.006
6. Wolf FA, Angerer P, Theis FJ. SCANPY: large-scale single-cell gene expression data analysis. *Genome Biol*. Feb 6 2018;19(1):15. doi:10.1186/s13059-017-1382-0
7. Luecken MD, Theis FJ. Current best practices in single-cell RNA-seq analysis: a tutorial. *Mol Syst Biol*. Jun 19 2019;15(6):e8746. doi:10.15252/msb.20188746
8. Hie B, Peters J, Nyquist SK, Shalek AK, Berger B, Bryson BD. Computational Methods for Single-Cell RNA Sequencing. *Annual Review of Biomedical Data Science*. 2020/07/20 2020;3(1):339-364. doi:10.1146/annurev-biodatasci-012220-100601
9. Zheng GX, Terry JM, Belgrader P, et al. Massively parallel digital transcriptional profiling of single cells. *Nat Commun*. Jan 16 2017;8:14049. doi:10.1038/ncomms14049
10. Tirosh I, Izar B, Prakadan SM, et al. Dissecting the multicellular ecosystem of metastatic melanoma by single-cell RNA-seq. *Science*. Apr 8 2016;352(6282):189-96. doi:10.1126/science.aad0501
11. Becht E, McInnes L, Healy J, et al. Dimensionality reduction for visualizing single-cell data using UMAP. *Nat Biotechnol*. Dec 3 2018;doi:10.1038/nbt.4314
12. Traag VA, Waltman L, van Eck NJ. From Louvain to Leiden: guaranteeing well-connected communities. *Sci Rep*. Mar 26 2019;9(1):5233. doi:10.1038/s41598-019-41695-z
13. The Gene Ontology resource: enriching a GOld mine. *Nucleic Acids Res*. Jan 8 2021;49(D1):D325-d334. doi:10.1093/nar/gkaa1113
14. Ashburner M, Ball CA, Blake JA, et al. Gene ontology: tool for the unification of biology. The Gene Ontology Consortium. *Nat Genet*. May 2000;25(1):25-9. doi:10.1038/75556
15. Tanaka Y, Cakir B, Xiang Y, Sullivan GJ, Park IH. Synthetic Analyses of Single-Cell Transcriptomes from Multiple Brain Organoids and Fetal Brain. *Cell Rep*. Feb 11 2020;30(6):1682-1689.e3. doi:10.1016/j.celrep.2020.01.038
16. Pollen AA, Bhaduri A, Andrews MG, et al. Establishing Cerebral Organoids as Models of Human-Specific Brain Evolution. *Cell*. Feb 7 2019;176(4):743-756.e17. doi:10.1016/j.cell.2019.01.017

17. Chen W, Teschendorff AE. Estimating Differentiation Potency of Single Cells Using Single-Cell Entropy (SCENT). *Methods Mol Biol*. 2019;1935:125-139. doi:10.1007/978-1-4939-9057-3_9

18. Teschendorff AE, Enver T. Single-cell entropy for accurate estimation of differentiation potency from a cell's transcriptome. *Nat Commun*. Jun 1 2017;8:15599. doi:10.1038/ncomms15599

19. Pellegrini L, Bonfio C, Chadwick J, Begum F, Skehel M, Lancaster MA. Human CNS barrier-forming organoids with cerebrospinal fluid production. *Science*. Jul 10 2020;369(6500)doi:10.1126/science.aaz5626

20. Heberle H, Meirelles GV, da Silva FR, Telles GP, Minghim R. InteractiVenn: a web-based tool for the analysis of sets through Venn diagrams. *BMC Bioinformatics*. May 22 2015;16(1):169. doi:10.1186/s12859-015-0611-3

21. Mi H, Ebert D, Muruganujan A, et al. PANTHER version 16: a revised family classification, tree-based classification tool, enhancer regions and extensive API. *Nucleic Acids Res*. Jan 8 2021;49(D1):D394-d403. doi:10.1093/nar/gkaa1106

22. Jassal B, Matthews L, Viteri G, et al. The reactome pathway knowledgebase. *Nucleic Acids Res*. Jan 8 2020;48(D1):D498-d503. doi:10.1093/nar/gkz1031

23. Virtanen P, Gommers R, Oliphant TE, et al. SciPy 1.0: fundamental algorithms for scientific computing in Python. *Nat Methods*. Mar 2020;17(3):261-272. doi:10.1038/s41592-019-0686-2

24. Raudvere U, Kolberg L, Kuzmin I, et al. g:Profiler: a web server for functional enrichment analysis and conversions of gene lists (2019 update). *Nucleic Acids Res*. Jul 2 2019;47(W1):W191-w198. doi:10.1093/nar/gkz369

25. Fernandes HJR, Patikas N, Foskolou S, et al. Single-Cell Transcriptomics of Parkinson's Disease Human In Vitro Models Reveals Dopamine Neuron-Specific Stress Responses. *Cell Rep*. Oct 13 2020;33(2):108263. doi:10.1016/j.celrep.2020.108263